ROYAL SOCIETY OF CHEMISTRY

COMMUNICATION

Check for updates

Constructing semiconductive crystalline microporous materials by Coulomb interactions†

Guan-E Wang, Ming-Shui Yao, Min-Lan Cai, Jing-Wei Xiu, Yan-Zhou Li, Gang Xu [ID] * and Guo-Cong Guo [ID] *

Crystalline materials possessing both porous and conductive properties would create a great opportunity for novel electrical applications in fuel cells, batteries and sensors. However, these kinds of materials are rarely reported. Here, we report a new type of conducting porous crystalline material constructed by long distance Coulomb interactions among inorganic and organic components. The compound in this work shows a microporous structure, typical semiconductive properties, selective adsorption and an interesting electrical response to methanol and ethanol.

Crystalline microporous materials possess a large surface area, a crystalline ordered structure and highly regularized pores that have potential applications for selective catalysis,[1] gas separation,[2] gas adsorption and storage,[3] ionic conductivity,[4] *etc.* At present, crystalline microporous materials can be mainly divided into two types according to the bonding interactions among their components (Scheme 1). The most reported one is constructed by "hard interactions", which possess bonding energies as high as several hundreds of kJ mol^{-1}, including metal–organic

frameworks (MOFs) by coordination bonding[5] and covalent organic frameworks (COFs) by covalent bonding.[6] The other type is constructed by "soft interactions", where bonding energies are one order of magnitude lower than those of hard interactions, like hydrogen-bonded organic frameworks (HOFs) by hydrogen bonding interactions,[7] and porous molecular crystals by van der Waals interactions and halogen bonding interactions.[8] The porous materials built by soft interactions often manifest unique and useful properties. For example, they can change their crystal structure when stimulated by mechanical, thermal or light stimuli, which is very attractive for switching and actuator applications.[9] On the other hand, porous materials constructed by soft interactions are normally in a metastable state; they have a tendency to become dense materials. Therefore, it is not surprising that although soft interactions exist in a large number of materials, the porous structures constructed by soft interactions are rarely reported, but are extremely desired.

Recently, endowing crystalline porous materials with electrical conduction properties has become a newly emerging research field. Porosity combined with conductivity would create a great opportunity to extend the applications to gas/vapor sensors, porous field-effect transistors, supercapacitors, fuel cells, Li ion batteries, and resistive memory devices.[10] For example, our group and the Dincă group have successfully used conductive MOFs as the sole electrode material to fabricate solid-state supercapacitors which show surface area-normalized capacitances beyond those of most porous carbon-based devices, such as those composed of activated carbon and carbon nanotubes, respectively.[11] Talin, Allendorf and their co-workers reported the first thermoelectric MOF material which possesses a Seebeck coefficient at room temperature comparable to that of the best organic materials, and exceeds that of Bi_2Te_3.[12] However, the design and synthesis of this kind of multi-functional material is still a big challenge.
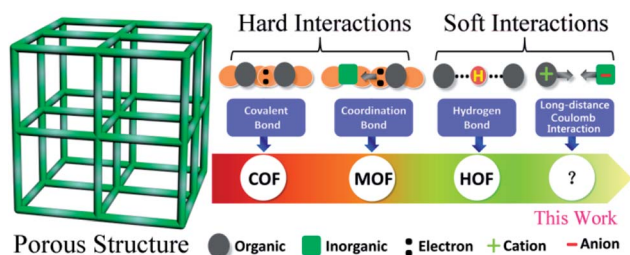
Scheme 1 Different types of crystalline microporous material.

State Key Laboratory of Structural Chemistry, Fujian Institute of Research on the Structure of Matter, Chinese Academy of Sciences, Yangqiao West Road 155#, Fuzhou, Fujian 350002, P. R. China. E-mail: gxu@fjirsm.ac.cn; gcguo@fjirsm.ac.cn

† Electronic supplementary information (ESI) available. CCDC 917236. For ESI and crystallographic data in CIF or other electronic format see DOI: 10.1039/c7ta05805e

Results and discussion

Here, we show a new way to design crystalline conductive porous materials by long distance Coulomb interactions (the

This journal is © The Royal Society of Chemistry 2017

J. Mater. Chem. A, 2017, 5, 18409–18413 | 18409

distance between two charged sites is longer than the sum of their ionic diameters). As a proof of concept, two micro-porous compounds, (organic)$_n$(Pb$_2$I$_6$)$_n$ (organic = [Cu(2,2'-bipy)$_2$I]$^+$ for **1** and [(H$_2$EDAB)$^{2+}$] for **2**; 2,2'-bipy = 2,2'-bipyridine, [(H$_2$EDAB)$^{2+}$] = Et$_2$HNC$_6$H$_4$C$_6$H$_4$NHEt$_2$) were synthesized. Although a quasi-1D metal halide chain based hybrid compound, which can reversibly adsorb and desorb a small number of water molecules, has been reported by M. Yamashita,[13] this study is the first time it is shown that Coulomb interactions are an effective physical force to form pore structures with open-window sizes approaching the nanoscale. Decreasing the distance between positively/negatively charged sites and increasing the number of Coulomb interaction sites were achieved by rationally designing the structures of organic cations, which substantially strengthen the Coulomb forces among the components and therefore enhance the stability of (organic)$_n$(Pb$_2$I$_6$)$_n$. Interestingly, by using iodioplumbate chains as the inorganic components, multi-functional materials were obtained. Compounds **1** and **2** show not only nanoscale porosity but also semiconducting properties and an enormous electrical response to methanol and ethanol.

Dark green crystals of compound **1** crystallize in the $P\bar{1}$ space group with inorganic infinite chains [(Pb$_2$I$_6$)$^{2-}$]$_\infty$ and counter ions [Cu(2,2'-bipy)$_2$I]$^+$ (Fig. 1a), as reported previously.[14] Each [Cu(2,2'-bipy)$_2$I]$^+$ organic monocation interacts with two neighboring ones through face-to-face π–π stacking interactions between the aromatic rings of 2,2'-bipy ligands to form 1-D [Cu(2,2'-bipy)$_2$I]$^+$ supramolecular chains extended along the b axis (Fig. S1†). The [(Pb$_2$I$_6$)$^{2-}$]$_\infty$ anionic chains and [Cu(2,2'-bipy)$_2$I]$^+$ cationic chains alternately stack with each other through Coulomb interactions to form 1-D channels along the c axis with an opening window of ∼7.5 Å, which are embedded with DMF and water molecules. The shortest contacts between the independent charge centers of [Cu(2,2'-bipy)$_2$I]$^+$

monocations and [(Pb$_2$I$_6$)$^{2-}$]$_\infty$ anionic chains are Cu1···I1 (8.239 Å), Cu1···I2 (5.923 Å) and Cu1···I3 (5.787 Å) (Table S1†), respectively, which are significantly longer than the sum of their ionic diameters and form weak Coulomb interactions among them. The structure of **1** can only stay stable up to 80 °C. After that, the guest molecules in **1** are released due to thermal induction and the porous structure of **1** changes to a close packing form by single crystal to single crystal transformation (Fig. 2a and S2†). If the organic component in **1** is designed from bulky to slim shapes and from monocations instead of multi-charged cations, the distance between the organic and inorganic components will decrease and the Coulomb interactions will become stronger, which should substantially enhance the stability of the material.

The structure of **2** also contains [(Pb$_2$I$_6$)$^{2-}$]$_\infty$ chains. In contrast, compound **2** contains (H$_2$EDAB)$^{2+}$, with a dication of a slim shape, functioning as organic counter ions (Fig. 1b). Compound **2** crystallizes in the $P\bar{4}2_1c$ space group. Along the c axis, neighboring organic (H$_2$EDAB)$^{2+}$ dications are packed in a crossed-maner to form organic columns (Fig. S3†). [(Pb$_2$I$_6$)$^{2-}$]$_\infty$ chains and (H$_2$EDAB)$^{2+}$ dication columns in **2** stack together through enhanced Coulomb interactions to form 1-D nano-channels along the c direction with an opening window of ∼1.0 nm (Fig. 1b and S3†). It is found that there is almost no residual electron density in the channels, indicating the empty micro-porous structure of **2**. The channels occupy 22.3% of the crystal volume of **2** as calculated by the program PLATON. The introduction of hydrophobic groups (*e.g.* methyl or ethyl) to the channel will enhance the water resistance of the structure.[15] It is worth noting that all of the ethyl groups in H$_2$EDAB protrude into the channels and create a hydrophobic environment. The closest I···N distance is 4.417 Å (I1···N1) and the closest I···π distance is 3.909 Å (I2···C2), which exceed the sums of the relevant van der Waals radii (I···N = 3.53 Å and I···C = 3.68 Å),
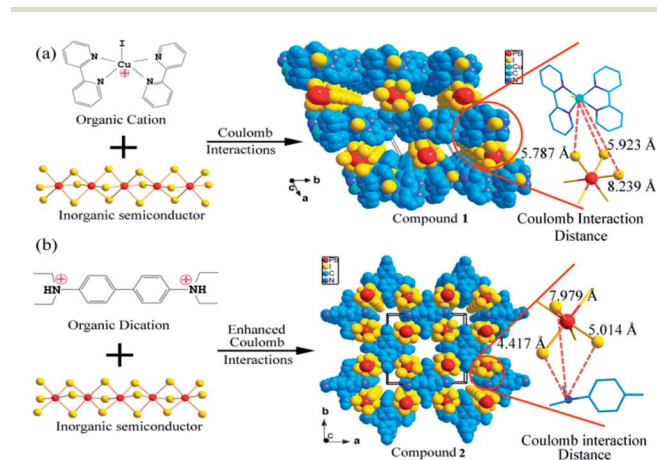

Fig. 1 (a) [Cu(2,2'-bipy)$_2$I]$^+$ organic monocation, [(Pb$_2$I$_6$)$^{2-}$]$_\infty$ anionic chain and structure of compound **1** with the DMF molecules, water molecules, and hydrogen atoms being omitted for clarity. (b) (H$_2$EDAB)$^{2+}$ organic dication, [(Pb$_2$I$_6$)$^{2-}$]$_\infty$ anionic chain and structure of compound **2** with the hydrogen atoms being omitted for clarity. The insets show the shortest contacts between the charge centers of the organic cation and the inorganic anion.
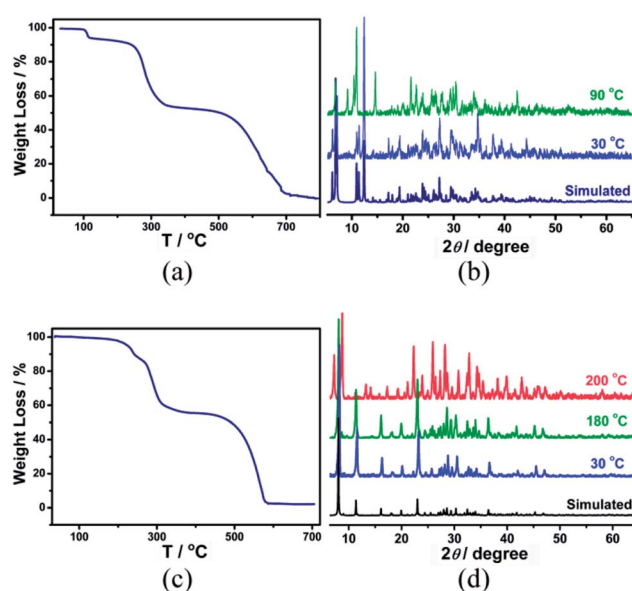

Fig. 2 TGA curves of **1** (a) and **2** (c). Variable-temperature PXRD patterns of **1** (b) and **2** (d).

18410 | *J. Mater. Chem. A*, 2017, 5, 18409–18413

This journal is © The Royal Society of Chemistry 2017

suggesting there are no halogen bonding interactions, but only Coulomb interactions among inorganic and organic components. The shortest contacts between the $(H_2EDAB)^{2+}$ dications and the $[(Pb_2I_6)^{2-}]_\infty$ anionic chains are $N1\cdots I1$ (4.417 Å), $N1\cdots I2$ (5.014 Å) and $N1\cdots I3$ (7.979 Å), respectively (Table S1†). According to Coulomb's law, the magnitude of the electrostatic force is inversely proportional to the square of the distance between two point charges. Although it is not precise to directly take $[(Pb_2I_6)^{2-}]_\infty$, $[Cu(2,2'-bipy)_2I]^+$ and $(H_2EDAB)^{2+}$ as point charges, the interactions in **1** and **2** should still follow Coulomb's law. The shortest distances among the charge centers in **2** are shorter than those in **1**, indicating much stronger Coulomb interactions in **2**. Moreover, each $[H_2EDAB]^{2+}$ dication in **2** supplies two Coulomb interaction sites. Therefore, the Coulomb interactions in **2** are greatly enhanced. There is no obvious change observed in the PXRD pattern of **2** before 180 °C (Fig. 2c and d), suggesting that **2** can retain its porous structure under a temperature of 100 °C, higher than that of **1**. Notably, compound **2** represents the first Coulombic interaction stabilized structure that possesses permanent nanoscale pores.

Since compound **1** can not be thermally activated, gas and vapor adsorption measurements were only performed with **2**. Before carrying out adsorption experiments, the crystals of **2** (100 mg) were immersed in CH_3OH for three days, then degassed automatically in a Micromeritics ASAP 2020-M at 60 °C for 24 h to generate the activated crystals of **2**. The PXRD data of **2** after activation and adsorption measurements indicate that its porous crystal structure is robust (Fig. S4†). Compound **2** shows no obvious adsorption of N_2, which is common in porous materials and might be due to weak interactions between the pore surface and N_2.[16] The CO_2 uptake values were 1307 cm^3 mol^{-1} (2.29 mg g^{-1}) at 273 K, and 481 cm^3 mol^{-1} (0.84 mg g^{-1}) at 298 K (Fig. S5†), respectively. This selective CO_2 adsorption over N_2 adsorption may be ascribed to the special quadrupole moment of CO_2 (13.4 cm^2), which has been attested to be a big contributor to the high affinity between CO_2 molecules and the compound skeleton and the CO_2-adsorption capability.[17] As shown in Fig. 3, the amount of the adsorbed ethanol and methanol in **2** sharply increases below $0.2P/P_0$ and then gradually increases by increasing the relative pressure at 298 K. As shown in Fig. 3 the adsorption amounts are 46 and 42 mg g^{-1} for ethanol and methanol, respectively, which are smaller than the calculated values (136 and 95 mg g^{-1} for ethanol and methanol, respectively). The result means that the adsorbed gas does not fully occupy the channel. These observations clearly indicate the microporous structure feature of **2**. It is also noticed that the empty channel of **2** shows hydrophobic properties, resulting in the uptake amount of methanol and ethanol being over 7 times higher than that of water.

Crystalline microporous materials with electronic conducting properties are extremely desired but rare.[18] Notably, iodoplumbate based hybrids are well-known semiconducting materials.[19] Therefore, the $[(Pb_2I_6)^{2-}]_\infty$ chains in (organic)$_n$ $(Pb_2I_6)_n$ may act as conductive functional pathways for charge transport. The temperature-dependent I–V curve measurements for the single crystals of **1** and **2** with a two-terminal-probe
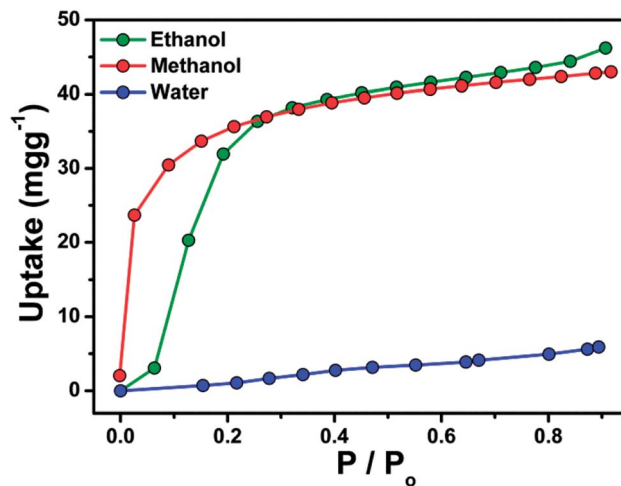

Fig. 3 Methanol, ethanol and water adsorption isotherms for **2**. Saturation pressures (P_0) of ethanol, methanol and water are 7.80, 16.83, and 3.17 kPa, respectively.

direct current method along the extension direction of $[(Pb_2I_6)^{2-}]_\infty$ chains are shown in Fig. 4 and S6.† As shown in Fig. 4c and d, the log σ of **1** and **2** linearly increases with decreasing $1/T$ ($T = 293$ to 353 K for **1**; $T = 303$ to 423 K for **2**), demonstrating their semiconductive features. At room temperature, the conductivity of **1** (2.50×10^{-10} S cm^{-1}) is

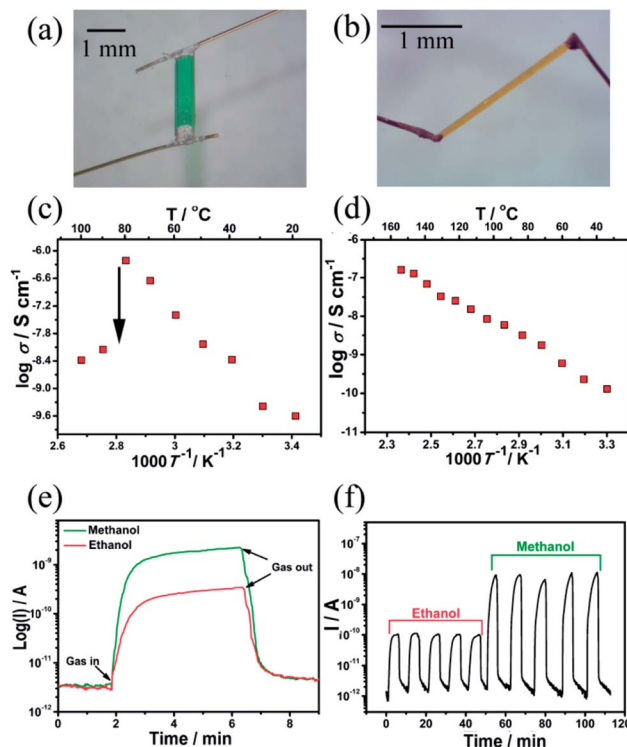**Fig. 4** Photographs of **1** (a) and **2** (b) single crystals for electronic study. log σ *versus* temperature plot for **1** (c) and **2** (d). Room temperature gas sensitive properties of **2**: response–recovery curves of **2** to methanol and ethanol, respectively (e); repeated response of **2** to methanol and ethanol, respectively (f).

similar to that of **2** (1.30×10^{-10} S cm^{-1}) due to their similar band structures in theoretical calculations (for details see Section 6, Fig. S7 and S8, ESI†). Compound **1** increases its conductivity to 6.10×10^{-7} S cm^{-1} at 80 °C, but this sharply decreases by 2 orders of magnitude to 4.93×10^{-9} S cm^{-1} in the temperature range of 80 to 90 °C (Fig. 4c), owing to the collapse of the structure. In contrast, the conductivity of **2** keeps increasing linearly to 1.61×10^{-7} S cm^{-1} up to 150 °C (Fig. 4d). All of the above conductivity values fall in the range of typical semiconductive materials, and are comparable to those of other haloplumbate(II) based hybrids.[20]

Compound **2** is electrically sensitive to the vapour of methanol and ethanol. The single crystal of **2** was attached with two gold paste electrodes and then its electrical response to methanol and ethanol was evaluated with our previously reported method.[21] The experiments were carried out by placing the crystal electrode in a sealed quartz chamber and monitoring the corresponding resistance in the vapor of methanol or ethanol with dry air as the carrier gas. A stable baseline current was established under dry air flow, and a fast increase in current was observed upon exposure to methanol and ethanol vapor (Fig. 4e). The current showed a 5 or 4 orders of magnitude increment under saturated methanol and ethanol vapor, respectively (Fig. S9†). The current level was recovered when we replaced the vapor with dry air. The $\log(R_{air}/R_{gas} - 1)$ has a good linear relationship with $\log$(concentration) in a wide range (for the detailed calculations see Section 7, Fig. S9, ESI†). The detection limits for methanol and ethanol are 2.4×10^4 and 1.8×10^4 ppm, respectively. The reversible change in current was reproducible over more than 5 cycles (Fig. 4f). The explosion limits of methanol and ethanol are 6×10^4 to 3.65×10^5 and 4.3×10^4 to 1.9×10^5 ppm, respectively. Therefore, compound **2** has the potential to be an explosives monitoring material as its detection limits were just within the scope of the explosion limit of methanol and ethanol.

Conclusions

In summary, for the first time, we have demonstrated that a robust porous structure could be constructed by long distance Coulomb interactions. Moreover, the strategy to improve the stability of this type of porous structure by optimizing the shape and increasing the Coulomb interaction sites of the organic components has been revealed. Utilizing electrically active haloplumbates as the inorganic functional component endowed the materials with not only typical semiconductive behavior but also a high electrical response to saturated methanol and ethanol vapor (5 and 4 orders of magnitude resistance change, respectively). The electrical properties of the materials shown in this work have the potential to be optimized by: (1) using other one dimensional or two dimensional inorganic components with high conductivity, such as M(L)$_n$ or MML (M = Sn, Pt, Pb, *etc.*; L = halide, cyanide, *etc.*)[22] to replace the iodoplumbate chain in this work; (2) incorporating extended conjugated organic molecules, such as the derivatives of TCNQ, TTF, and phthalocyanin, that may achieve sufficient π–π interactions to build additional pathways for charge carrier transport; (3) doping guest molecules into the porous structure. Therefore, our work may shed light on designing and preparing new types of crystalline material with both high porosity and good conductivity.

Conflicts of interest

There are no conflicts to declare.

Acknowledgements

Notes and references

1 (a) H. L. Jiang, B. Liu, T. Akita, M. Haruta, H. Sakurai and Q. Xu, *J. Am. Chem. Soc.*, 2009, **131**, 11302–11303; (b) M. Ding, S. Chen, X. Q. Liu, L. B. Sun, J. Lu and H. L. Jiang, *ChemSusChem*, 2017, **10**, 1898–1903; (c) J. M. Falkowski, T. Sawano, T. Zhang, G. Tsun, Y. Chen, J. V. Lockard and W. Lin, *J. Am. Chem. Soc.*, 2014, **136**, 5213–5216.

2 (a) J. Li, J. Sculley and H. Zhou, *Chem. Rev.*, 2012, **112**, 869–932; (b) H. L. Jiang, Y. Tatsu, Z. H. Lu and Q. Xu, *J. Am. Chem. Soc.*, 2010, **132**, 5586–5587; (c) A. Chakraborty, S. Roy, M. Eswaramoorthy and T. K. Maji, *J. Mater. Chem. A*, 2017, **5**, 8423–8430; (d) B. Li, H.-M. Wen, Y. Cui, W. Zhou, G. Qian and B. Chen, *Adv. Mater.*, 2016, **28**, 8819–8860.

3 (a) C. X. Chen, Z. W. Wei, J. J. Jiang, S. P. Zheng, H. P. Wang, Q. F. Qiu, C. C. Cao, D. Fenske and C. Y. Su, *J. Am. Chem. Soc.*, 2017, **139**, 6034–6037; (b) H. Furukawa, K. E. Cordova, M. O'Keeffe and O. M. Yaghi, *Science*, 2013, **341**, 1230444–1230456; (c) W. Lu, Z. Wei, D. Yuan, J. Tian, S. Fordham and H. C. Zhou, *Chem. Mater.*, 2014, **26**, 4589–4597.

4 (a) T. Yamada, M. Sadakiyo and H. Kitagawa, *J. Am. Chem. Soc.*, 2009, **131**, 3144–3145; (b) J. M. Taylor, R. Vaidhyanathan, S. S. Iremonger and G. K. H. Shimizu, *J. Am. Chem. Soc.*, 2012, **134**, 14338–14340; (c) S. Horike, S. Shimomura and S. Kitagawa, *Nat. Chem.*, 2009, **1**, 695–704.

5 (a) M. Zhang, Y. P. Chen, M. Bosch, T. Gentle III, K. Wang, D. Feng, Z. U. Wang and H. C. Zhou, *Angew. Chem., Int. Ed.*, 2014, **53**, 815–818; (b) Z. Hao, G. Yang, X. Song, M. Zhu, X. Meng, S. Zhao, S. Song and H. Zhang, *J. Mater. Chem. A*, 2014, **2**, 237–244; (c) J. Zhang, P. Q. Liao, H. L. Zhou, R. B. Lin and X. M. Chen, *Chem. Soc. Rev.*, 2014, **43**, 5789–5814; (d) G. C. Lv, P. Wang, Q. Liu, J. Fan, K. Chen and W. Y. Sun, *Chem. Commun.*, 2012, **48**, 10249–10251; (e) D. Liu, J. P. Lang and B. F. Abrahams, *J. Am. Chem. Soc.*, 2011, **133**, 11042–11045; (f) D. T. Tian, Q. Chen,

Y. Li, Y. H. Zhang, Z. Chang and X. H. Bu, *Angew. Chem., Int. Ed.*, 2014, **53**, 837–841; (*g*) T. Zheng, Z. Yang, D. Gui, Z. Liu, X. Wang, X. Dai, S. Liu, L. Zhang, Y. Gao, L. Chen, D. Sheng, Y. Wang, J. Diwu, J. Wang, R. Zhou, Z. Chai, T. E. Albrecht-Shmitt and S. Wang, *Nat. Commun.*, 2017, **8**, 15369.

6 (*a*) C. Qian, Q. Y. Qi, G. F. Jiang, F. Z. Cui, Y. Tian and X. Zhao, *J. Am. Chem. Soc.*, 2017, **139**, 6736–6743; (*b*) Y. B. Zhang, J. Su, H. Furukawa, Y. Yun, F. Gándara, A. Duong, X. Zou and O. M. Yaghi, *J. Am. Chem. Soc.*, 2013, **135**, 16336–16339; (*c*) S. Chandra, T. Kundu, K. Dey, M. Addicoat, T. Heine and R. Banerjee, *Chem. Mater.*, 2016, **28**, 1489–1494.

7 (*a*) F. Hu, C. Liu, M. Wu, J. Pang, F. Jiang, D. Yuan and M. Hong, *Angew. Chem., Int. Ed.*, 2017, **56**, 2101–2104; (*b*) T. Hasell, S. Y. Chong, K. E. Jelfs, D. J. Adams and A. I. Cooper, *J. Am. Chem. Soc.*, 2012, **134**, 588–598; (*c*) J. Lü, P. K. Cristina, S. Mikhail, N. H. Alsmail, Y. Yan, S. Yang, W. Lewis, E. Bichoutskaia, C. C. Tang, A. J. Blake, R. Cao and M. Schröder, *J. Am. Chem. Soc.*, 2014, **136**, 12828–12831.

8 (*a*) P. Sozzani, S. Bracco, A. Comotti, L. Ferretti and R. Simonutti, *Angew. Chem., Int. Ed.*, 2005, **44**, 1816–1820; (*b*) F. C. Pigge, V. R. Vangala, P. P. Kapadia, D. C. Swenson and N. P. Rath, *Chem. Commun.*, 2008, 4726–4728.

9 (*a*) M. E. Brown and M. D. Hollingsworth, *Nature*, 1995, **376**, 323; (*b*) R. Kitaura, K. Seki, G. Akiyama and S. Kitagawa, *Angew. Chem., Int. Ed.*, 2003, **42**, 428–431.

10 (*a*) V. Stavila, A. A. Talin and M. D. Allendorf, *Chem. Soc. Rev.*, 2014, **43**, 5994–6010; (*b*) G. Wu, J. Huang, Y. Zang, J. He and G. Xu, *J. Am. Chem. Soc.*, 2017, **139**, 1360–1363; (*c*) Q. Wang, X. Feng, S. Wang, N. Song, Y. Chen, W. Tong, Y. Han, L. Yang and B. Wang, *Adv. Mater.*, 2016, **28**, 5837–5843; (*d*) I. Stassen, N. Burtch, A. Talin, P. Falcaro, M. Allendorf and R. Ameloot, *Chem. Soc. Rev.*, 2017, **46**, 3185–3241; (*e*) L. Sun, M. G. Campbell and M. Dincă, *Angew. Chem., Int. Ed.*, 2016, **55**, 2–16; (*f*) T. Panda and R. Banerjee, *Proc. Natl. Acad. Sci., India, Sect. A*, 2014, **84**, 331–336; (*g*) L. Pan, Z. Ji, X. Yi, X. Zhu, X. Chen, J. Shang, G. Liu and R. W. Li, *Adv. Funct. Mater.*, 2015, **25**, 2677–2685.

11 (*a*) W. H. Li, K. Ding, H. R. Tian, M. S. Yao, B. Nath, W. H. Deng, Y.-B. Wang and G. Xu, *Adv. Funct. Mater.*, 2017, **27**, 1702067; (*b*) D. Sheberla, J. C. Bachman, J. S. Elias, C. J. Sun, Y. S. Horn and M. Dincă, *Nat. Mater.*, 2017, **16**, 220–224.

12 K. J. Erickson, F. Léonard, V. Stavila, M. E. Foster, C. D. Spataru, R. E. Jones, B. M. Foley, P. E. Hopkins, M. D. Allendorf and A. A. Talin, *Adv. Mater.*, 2015, **27**, 3453–3459.

13 H. Iguchi, S. Takaishi, H. Miyasaka, M. Yamashita, H. Matsuzaki, H. Okamoto, H. Tanaka and S. Kuroda, *Angew. Chem., Int. Ed.*, 2010, **49**, 552–555.

14 G. E. Wang, G. Xu, P. X. Li, S. H. Wang, M. S. Wang and G. C. Guo, *CrystEngComm*, 2013, **15**, 2579–2582.

15 (*a*) D. Ma, Y. Li and Z. Li, *Chem. Commun.*, 2011, **47**, 7377–7379; (*b*) I. Gill and R. Valivety, *Angew. Chem., Int. Ed.*, 2000, **39**, 3801–3804; (*c*) L.-K. Wu, J.-M. Hu and J.-Q. Zhang, *J. Mater. Chem. A*, 2013, **1**, 14471–14475.

16 (*a*) J. Liu, P. K. Thallapally, B. P. McGrail, D. R. Brown and J. Liu, *Chem. Soc. Rev.*, 2012, **41**, 2308–2322; (*b*) J. R. Li, Y. Ma, M. C. McCarthy, J. Sculley, J. Yu, H. K. Jeong, P. B. Balbuena and H. C. Zhou, *Coord. Chem. Rev.*, 2011, **255**, 1791–1823.

17 (*a*) F. Luo, C. B. Fan, M. B. Luo, X. L. Wu, Y. Zhu, S. Z. Pu, W.-Y. Xu and G.-C. Guo, *Angew. Chem., Int. Ed.*, 2014, **53**, 9298–9301; (*b*) K. Sumida, D. L. Rogow, J. A. Mason, T. M. McDonald, E. D. Bloch, Z. R. Herm, T. H. Bae and J. R. Long, *Chem. Rev.*, 2012, **112**, 724–781; (*c*) S. R. Caskey, A. G. Wong-Foy and A. J. Matzger, *J. Am. Chem. Soc.*, 2008, **130**, 10870–10871.

18 (*a*) Y. Kobayashi, B. Jacobs, M. D. Allendorf and J. R. Long, *Chem. Mater.*, 2010, **22**, 4120–4122; (*b*) S. Bao, K. Otsubo, J. Taylor, Z. Jiang, L. Zheng and H. Kitagawa, *J. Am. Chem. Soc.*, 2014, **136**, 9292–9295.

19 D. B. Mitzi, *Chem. Mater.*, 2001, **13**, 3283–3298.

20 C. C. Stoumpos, C. D. Malliakas and M. G. Kanatzidis, *Inorg. Chem.*, 2013, **52**, 9019–9038.

21 M. S. Yao, W. X. Tang, G. E. Wang, B. Nath and G. Xu, *Adv. Mater.*, 2016, **28**, 5229–5234.

22 (*a*) K. Otsubo, Y. Wakabayashi, J. Ohara, S. Yamamoto, H. Matsuzaki, H. Okamoto, K. Nitta, T. Uruga and H. Kitagawa, *Nat. Mater.*, 2011, **10**, 291–295; (*b*) M. Mitsumi, T. Murase, H. Kishida, T. Yoshinari, Y. Ozawa, K. Toriumi, T. Sonoyama, H. Kitagawa and T. Mitani, *J. Am. Chem. Soc.*, 2001, **123**, 11179–11192; (*c*) M. Mitsumi, H. Ueda, K. Furukawa, Y. Ozawa, K. Toriumi and M. Kurmoo, *J. Am. Chem. Soc.*, 2008, **130**, 14102–14104; (*d*) M. Mitsumi, T. Nishitani, S. Yamasaki, N. Shimada, Y. Komatsu, K. Toriumi, Y. Kitagawa, M. Okumura, Y. Miyazaki, N. Górska, A. Inaba, A. Kanda and N. Hanasaki, *J. Am. Chem. Soc.*, 2014, **136**, 7026–7037.